AERODYNAMIC CHARACTERISTICS OF DEFLECTED SURFACES IN COMPRESSIBLE FLOWS

Kung-Ming Chung
Aerospace Science and Technology Research Center
National Cheng Kung University, Taiwan, ROC

Keywords: *convex corner, concave corner, incremental lift*

Abstract

An experimental study on the compressible convex-corner and concave-corner flows was conducted, which is related to the simplified model of upper and lower deflected surfaces. The interaction region and the characteristic pressures were obtained to get a quick estimation of the aerodynamic coefficients at subsonic speeds. The integration of surface pressure distributions was also performed. The incremental lift and lift-induced-drag coefficients increase with the deflection angle and the freestream Mach number, and the similarity parameter $M\eta$ appears to be a suitable parameter to characterize the aerodynamic coefficients. Substantial increase in lift-induced-drag coefficient is associated with the separated flow on the upper surface.

1 Introduction

The flap can be used as the high-lift device, in which a deflection downward results in the gain in lift at the given geometric angle of attack. For the influence of small flap deflections, a straight line from the leading to trailing edges of a symmetrical airfoil at zero angle of attack is treated as the fictitious chord line. The problem is reduced to a camber airfoil at an angle of attack. The incremental lift coefficient and moment coefficient about the aerodynamic center vary with the flap deflection, and can be predicted by thin-airfoil theory. The magnitudes are related to the distance of the hinge line behind the leading edge [1]. Note that the agreement between theory and experiment is poor due to the boundary layer effect. Furthermore, Bolonki and Gilyard [2] indicated that the deflected control surfaces could be used in combination to provide the variable camber control within the operational flight envelope of a civil aircraft. At cruise speeds, the benefits of variable camber using a simple trailing-edge control surface system could approach more than 10 percent in maximizing the lift-to-drag ratio, especially for nonstandard flight conditions. However, the critical Mach number, onset of boundary layer separation and drag are also strongly related to the allowable deflection of the control surfaces.

A simplified model of deflected control surface was studied by Chung [3-5]. On the upper deflected surface (or convex corner flow), strong upstream expansion and downstream compression are observed near the corner in the compressible flows. The interaction region can be scaled with the freestream Mach number and the convex-corner angle ($M^2\eta$). The boundary layer downstream of the corner is separated at $M^2\eta \geq 8.95$. The separation position moves slightly upstream while the reattachment position moves downstream with increasing convex-corner angle. On the lower deflected surface (or concave-corner flow), the flow decelerates upstream of the corner followed by the downstream acceleration. The characteristics of the flow, e.g. upstream compression, downstream expansion, and interaction region, are associated with the freestream Mach number and the concave-corner angle.

To characterize the aerodynamic performance of a deflected surface in compressible flows, the present study re-examined a turbulent boundary layer past the convex and concave corners at M = 0.64 and

0.83, Fig. 1. This investigation involved the analysis of mean pressure distributions of the convex- and concave-corner flows. The incremental lift and lift-induced-drag coefficients are estimated based on the characteristics and the integration of surface pressure distributions.

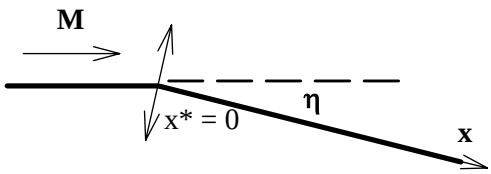

Fig. 1. Test Configuration

2 Experiment

2.1 Transonic Wind Tunnel

The transonic wind tunnel at Aerospace Science and Technology Research Center is a blowdown type, and operates in the Mach number from 0.2 to 1.4 at Reynolds numbers up to 20 million per meter [6]. Major components of the facility include compressors, air dryers, cooling water system, storage tanks and the tunnel. The dew point of high-pressure air through the dryers is maintained at -40°C under normal operation conditions. Air storage volume for the three storage tanks is up to 180 m^3 at 5.15 MPa. The test section is 600 mm square and 1500 mm long. In the present study, the test section was assembled with solid sidewalls and perforated top/bottom walls to reduce the background acoustic noise. The freestream Mach numbers were 0.64 and 0.83±0.01, and the stagnation pressure (p_o) and temperature (T_o) were 172±0.5 kPa and room temperature, respectively.

For the data acquisition system, the NEFF Instruments System 620 and the LeCroy waveform recorders were used. The test conditions were recorded by the NEFF system while the LeCroy 6810 waveform recorders were used for the pressure measurements. A host computer with CATALYST software controlled the setup of LeCroy waveform recorders through a LeCroy 8901A interface. All input channels were triggered simultaneously by using an input channel as the trigger source.

2.2 Test Model

The test model consists of a flat plate and an interchangeable instrumentation plate. The test model is 150 mm wide and 600 mm long, which is supported by a single sting mounted on the bottom wall of the test section. The concave corner with 3, 5, 7, 10, and 15-deg angles or the convex corner with 5, 10, 13, and 15-deg angles is located at 500 mm from the leading edge of the flat plate. One row of 19 holes, 6 mm apart and 2.5 mm in diameter, was installed along the centerline of each instrumentation plate perpendicular to the test surface. All the pressure transducers within the holes were flush-mounted to the test surface, and potted using silicone sealant. The side fences of the instrumentation plate were installed to prevent cross flow.

2.3 Experimental Techniques

For the surface pressure measurements, the Kulite (Model XCS-093-25A, B screen) pressure transducers powered by a TES Model 6102 power supply at 15.0 V were used. The outside diameter is 2.36 mm, and the sensing element is 0.97 mm in diameter. External amplifiers (Ecreon Model E713) were used to improve the signal-to-noise ratio. The typical sampling period is 5μs (200 kHz). Each data record possesses 131,072 data points for the statistical analysis. The data were divided into 32 blocks. The mean values of each block (4,096 data points) were calculated. Variations of the blocks are estimated to be 0.43 percent for the mean surface pressure coefficient ($C_p = (p_w-p_\infty)/q_\infty$), which is considered to be the uncertainty of experimental data.

For the characteristics of the incoming boundary layer, the Pitot pressure surveys were conducted at 25 mm upstream of the corner without the corner in place. The normalized velocity profiles appear to be full ($n \approx 7$-11 for the velocity power law). A study by Miau et al.

[7] further indicated that the transition of the boundary layer under the present test condition is close to the leading edge of the flat plate. This indicates turbulent flow at the measurement locations. The boundary layer thickness is estimated to be 7.3 and 7.1±0.2 mm for M = 0.64 and 0.83, respectively.

3 Results and Discussion

3.1 Interaction Region

Examples of the mean surface pressure coefficients C_p along the centerline of the instrumentation plates are shown in Fig. 2 ($x^* = x/\delta$). The solid symbol represents the mean pressure distributions on the upper surface of a deflected surface (or convex corner), while the hollow symbol is for the lower surface (or concave corner). It can be seen that the flows accelerate upstream of the convex corner followed by the compression. Stronger upstream expansion and downstream recompression are associated with increasing convex-corner angle, and the minimum pressure is observed near the corner. Nearly constant pressure gradients (upstream expansion and downstream compression) are observed for the subsonic expansion flows. For the transonic unseparated expansion flows ($M^2\eta \geq 6.14$), there are more intense pressure variations near the corner. Mild initial compression and larger interaction region are associated with the separated transonic expansion flows (M = 0.83 at η = 10- and 15-deg, Fig. 2b). On the lower surface, the pressure distributions of the concave-corner flow show similar in shape for all the test cases. The flows decelerate upstream of the concave corner followed by the expansion. The interaction region tends to expand in both upstream and downstream directions with larger concave-corner angle. Linear variations of upstream compression and downstream expansion are observed.

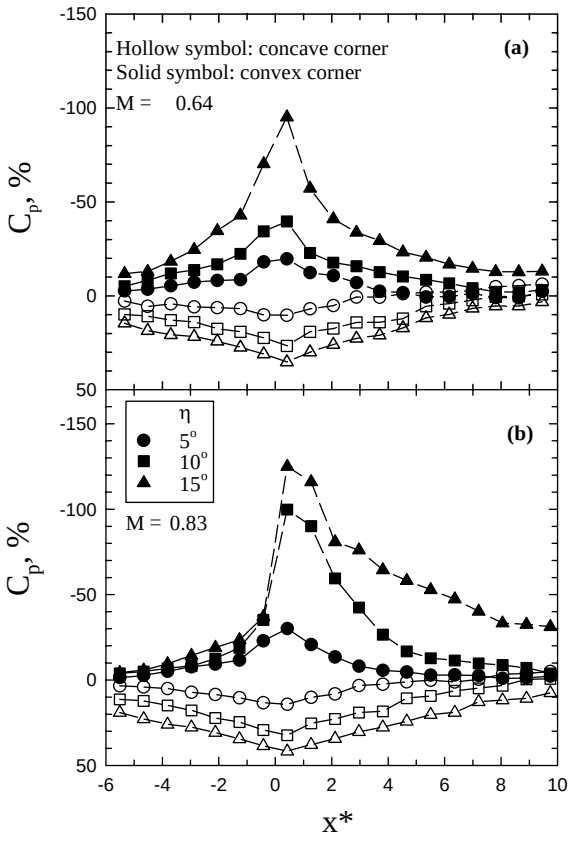

Fig. 2. Surface Pressure Distributions

To get a quick estimation of the incremental aerodynamic coefficients of a deflected surface near the corner, the present study re-examine the characteristics of the mean surface pressure distributions. These include the upstream and downstream influence regions, pressure gradients (the levels of expansion or compression), peak pressure near the corner and downstream pressure. For the upstream influence x^*_u, it can be determined as the intercept of the tangent to the maximum pressure gradient with the undisturbed surface pressure (or $C_p = 0$) [8]. The downstream influence x^*_d represents the distance for a disturbed boundary layer back to the equilibrium status, and can be estimated from the peak pressure near the corner to the intersection of the tangent through the downstream pressure data with the approximately equilibrium downstream pressure. Since the adequate equilibrium downstream pressure can only be approximately obtained, the estimation of the downstream influence

region is subjected to more uncertainty. In Fig. 3, the interaction length is scaled with $M^2\eta$ for the convex-corner flows [3] and with $M\eta$ for the concave-corner flows [5]. The test cases of transonic separated convex-corner flows are not included. It can be seen that the upstream influence and downstream influence regions appear to increase linearly with $M^2\eta$ or $M\eta$. Note that the extent of upstream influence region for the concave-corner flow is considerably more than that of the convex-corner flow. The difference of the downstream influence region is less significant.

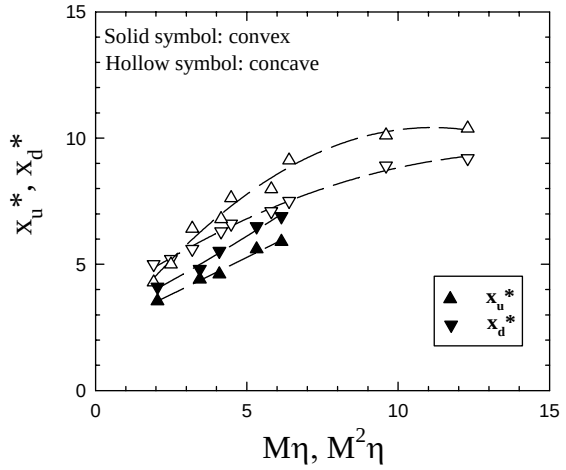

Fig. 3. Upstream/Downstream Influence

3.2 Characteristics of Pressure Distributions

Upstream expansion of the convex-corner flows is characterized as the mild initial expansion and stronger expansion near the corner (Fig. 2a). The levels of upstream initial expansion (dC_p/dx^*, Fig. 4a), which ranges from –0.10 to –0.02, decrease for the subsonic expansion flows and increase for the transonic expansion flows with $M^2\eta$. Stronger expansion is associated with increasing $M^2\eta$, particularly for the transonic expansion flows. Downstream of the convex corner, the compression is related to the type of expansion flows. For the attached flows, the levels of adverse pressure gradient (compression) increase for the subsonic expansion flows and decrease for the transonic expansion flows with $M^2\eta$. When the boundary layer is separated ($M^2\eta \geq 8.95$), variation of the initial compression downstream of the convex corner is minimized. Furthermore, the upstream compression and downstream expansion for the concave-corner flows are shown in Fig. 4b. The levels of upstream and downstream pressure gradient, which can also be scaled with $M^2\eta$, are considerably less than those of the convex-corner flows. This implies the major influence of the convex-corner flow (or upper surface) on the aerodynamic characteristics of a deflected surface. It is noted that the levels of pressure gradient approach to some equilibrium values at $M^2\eta \geq 7$ for the concave-corner flows.

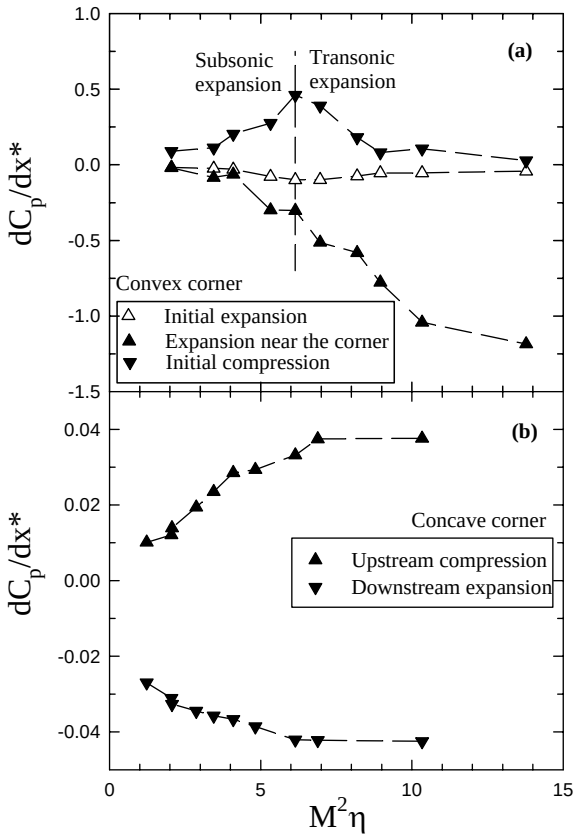

Fig. 4. Characteristics of Expansion and Compression

The peak pressure $C_{p,peak}$ near the corner and the downstream surface pressure $C_{p,d}$ are also required to estimate the aerodynamic characteristics of a deflected surface. Figure 5 shows that these characteristic pressures can be scaled with $M^2\eta$ or $M\eta$ for the convex-corner or the concave-corner flows, respectively. The peak pressure and downstream surface pressure of the convex corner flows are substantially decreased with increasing $M^2\eta$. The concave-

corner flows show the opposite trend with Mη, in which there is mild variation of the pressure levels. The increasing expansion for the convex-corner flows (upper surface) and stronger compression for the concave-corner flows (lower surface) imply the increment of the lift coefficient with $M^2\eta$ or Mη.

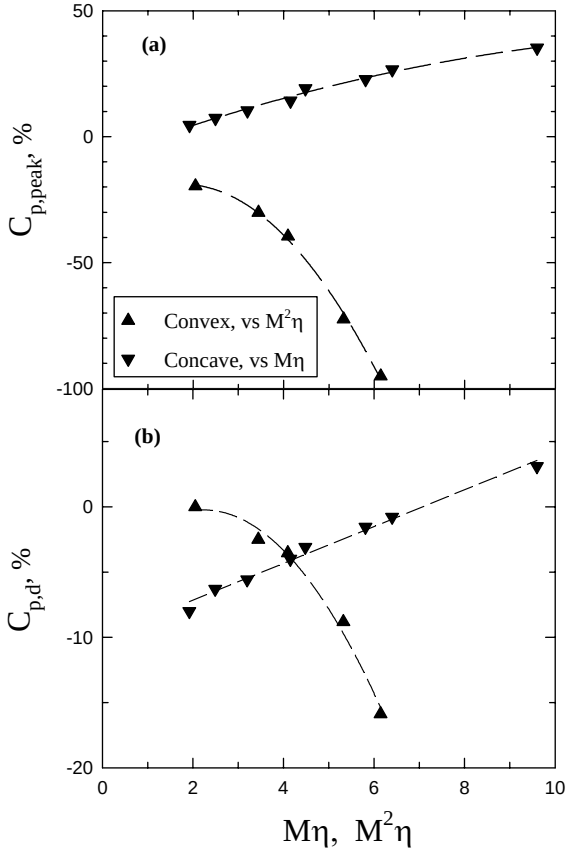

Fig. 5. Characteristic Pressures

3.3 Aerodynamic Characteristics

Kuethe and Chow [1] indicated that the incremental lift coefficient varies linearly with the flap deflection for incompressible flows. For the present study, the incremental lift and drag coefficients of the deflected surface (upper convex-corner surface and lower concave-corner surface) can be simply estimated by the interaction regions and characteristic pressures at subsonic speeds. The incremental lift coefficient Δc_L is up to 0.2, and appears to be a quadratic function of Mη in Fig. 6. The additional positive lift force also produces additional induced drag Δc_D, particularly at higher $M_\infty\eta$. The benefit with a simple deflected flap will thus decrease.

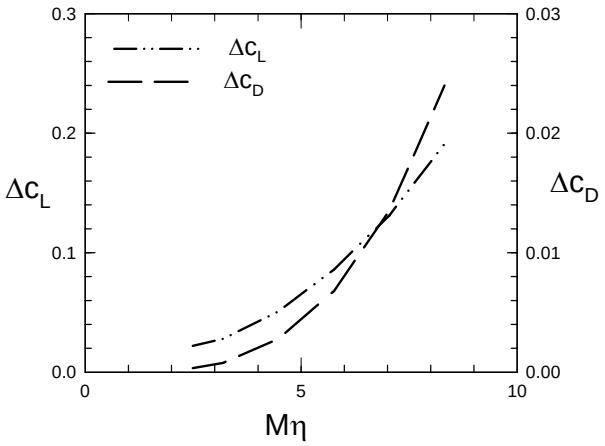

Fig. 6. Incremental Lift and Drag Estimated by Characteristics of Pressure Distributions, Subsonic Flows

Further, Δc_L and Δc_D (M = 0.64 and 0.83 at η = 5-, 10-, 15-deg) are estimated by the integration of pressure distributions on the upper and lower surfaces. Fig. 7a shows that Δc_L increases linearly with the deflection angle at M = 0.64 or 0.83. At a given deflection angle, higher Δc_L is observed at M = 0.83 than that at M = 0.64. This may correspond to the compressibility effect. It is also observed that variation of Δc_L with Mη coincides reasonably well for both testing Mach numbers. Estimation of the lift-induced-drag is shown in Fig. 7b. For the attached flows on the upper surface (convex-corner flows at Mη ≤ 9.6), Δc_D increases gradually with Mη. Substantial increase in Δc_D is observed with the separated convex-corner flow at Mη = 12.45 (or $M^2\eta$ = 10.33).

4 Conclusions

A simplified model of deflected surface was studied. At subsonic speeds, the incremental lift coefficient and lift-induced-drag coefficient can be estimated from the interaction region and the characteristic pressures reasonably well. Integration of the surface pressure distributions was also performed. The major effect on the aerodynamic characteristics corresponds to stronger pressure variations on the upper surface (or convex-corner flow). The effects of increasing deflection angle and freestream Mach

number are observed, and the increment varies with the similarity parameter Mη reasonably well. Substantial increase in the lift-induced-drag coefficient is associated with the transonic separated flow on the upper surface.

5 Acknowledgement

The research was under the support of National Science Council (NSC 90-2212-E-006-132). The support is gratefully acknowledged. The author also thanks the technical support of ASTRC/NCKU technical staffs with the experiments.

References

[1] Kuethe, A, and Chow, C. *Foundations of aerodynamics*. 3rd edition, John Wiley & Sons, Inc., 1976, pp.133-138.

[2] Bolonki, A, and Gilyard, G. *Estimated benefits of variable-geometry wing camber control for transport aircraft*. NASA TM-1999-206586, October 1999.

[3] Chung, K. Transition of subsonic and transonic expansion flows. *Journal of Aircraft*, Vol. 37, No. 6, pp. 1079-1082, 2000.

[4] Chung, K. Investigation on transonic convex-corner flows. *Journal of Aircraft*, Vol. 39, No. 6, pp. 1014-1018, 2002.

[5] Chung, K. An experimental study of compressible concave corner flows. Proceeding *2002 International Conference on the Methods of Aerophysics Research*, Novosibirsk, Russia, July 2002.

[6] Chung, K. *Development and calibration of ASTRC/ NCKU 600 mm x 600 mm transonic wind tunnel*. NSC 83-2212-E-006-141T, August 1994.

[7] Miau, J, Cheng, J, Chung, K, and Chou, J. The effect of surface roughness on the boundary layer transition. Proc. *7th International Symposium in Flow Modeling and Turbulent Measurement*, Tainan, Taiwan, ROC, ISFMTM98', pp. 609-616, 1998.

[8] Lu, F. *Fin generated shock-wave boundary layer interactions*. Ph.D. Dissertation, Penn State University, May 1988

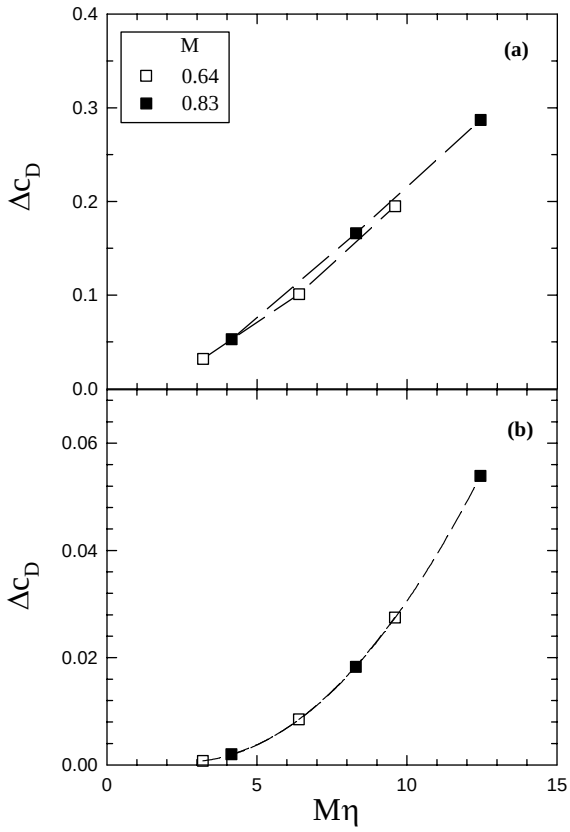

Fig. 7. Incremental Lift and Drag Estimated by the Integration of Surface Pressure